Adaptation of olfactory receptor abundances for efficient coding

Tiberiu Teşileanu[1,2], Simona Cocco[3], Rémi Monasson[4], and Vijay Balasubramanian[1,2]

[1]Initiative for the Theoretical Sciences, The Graduate Center, CUNY, New York, NY 10016
[2]David Rittenhouse Laboratories, University of Pennsylvania, Philadelphia, PA 19104
[3]Laboratoire de Physique Statistique, École Normale Supérieure and CNRS UMR 8550, PSL Research, UPMC Sorbonne Université, Paris, France
[4]Laboratoire de Physique Théorique, École Normale Supérieure and CNRS UMR 8550, PSL Research, UPMC Sorbonne Université, Paris, France

July 19, 2018

Abstract

Olfactory receptor usage is highly non-uniform, with some receptor types being orders of magnitude more abundant than others. We propose an explanation for this striking fact: the receptor distribution is tuned to maximally represent information about the olfactory environment in a little-studied regime of efficient coding that is sensitive to the global context of correlated sensor responses. This model predicts further that in mammals, where olfactory sensory neurons are replaced regularly, receptor abundances should continuously adapt to odor statistics. Indeed, experiments have found such changes in response to olfactory experience. These changes are mysteriously context-dependent, with increased exposure to odorants leading variously to increased, decreased or unchanged abundances of activated receptors. We show that efficient coding theory predicts precisely such a context-dependence when sensors are correlated. Finally, we demonstrate simple dynamical rules for neural birth and death processes that might provide a mechanism for receptor abundances to adapt optimally.

1 Introduction

The sensory periphery acts as a gateway between the outside world and the brain, shaping what an organism can learn about its environment. The gateway has a limited capacity (Barlow, 1961), restricting the amount of information that can be extracted to support behavior. On the other hand, signals in the natural world typically contain many correlations that limit the unique information that is actually present in different signals. The efficient-coding hypothesis, a key normative theory of neural circuit organization, puts these two facts together, suggesting that the brain mitigates the issue of limited sensory capacity by eliminating redundancies implicit in the correlated structure of natural stimuli (Barlow, 1961; van Hateren, 1992a). This idea has led to elegant explanations of

functional and circuit structure in the early visual and auditory systems (see, *e.g.,* (Laughlin, 1981; Atick and Redlich, 1990; van Hateren, 1992b; Olshausen and Field, 1996; Simoncelli and Olshausen, 2001; Fairhall et al., 2001; Lewicki, 2002; Ratliff et al., 2010; Garrigan et al., 2010; Tkacik et al., 2010; Hermundstad et al., 2014; Palmer et al., 2015; Salisbury and Palmer, 2016)). However, these classic studies lacked a way to test causality, where changes in the environment lead to adaptive changes in circuit composition or architecture. We propose that the olfactory system provides an avenue for such a causal test because receptor neuron populations in the mammalian nasal epithelium are regularly replaced, leading to the possibility that their abundances might adapt efficiently to the statistics of the environment.

In detail, the olfactory epithelium in mammals and the antennae in insects are populated with large numbers of olfactory sensory neurons (OSNs), each of which expresses a single kind of olfactory receptor. Each type of receptor binds to many different odorants, and each odorant activates many different receptors, leading to a complex encoding of olfactory scenes (Malnic et al., 1999). Olfactory receptors form the largest known gene family in mammalian genomes, with hundreds to thousands of members, owing perhaps to the importance that olfaction has for an animal's fitness (Buck and Axel, 1991; Chess et al., 1994; Tan et al., 2015). Independently-evolved large olfactory receptor families can also be found in insects (Missbach et al., 2014). Surprisingly, although animals possess diverse repertoires of olfactory receptors, their expression is actually highly non-uniform with some receptors occurring much more commonly than others (Rospars and Chambille, 1989; Ibarra-Soria et al., 2017). In addition, in mammals, the olfactory epithelium experiences neural degeneration and neurogenesis, resulting in replacement of the OSNs every few weeks (Monti Graziadei and Graziadei, 1979). The distribution of receptors resulting from this replacement has been found to have a mysterious dependence on olfactory experience (Schwob et al., 1992; Santoro and Dulac, 2012; Zhao et al., 2013; Dias and Ressler, 2014; Cadiou et al., 2014; Ibarra-Soria et al., 2017): increased exposure to ligands sometimes leads to more receptors, sometimes to fewer receptors, and sometimes has no effect. Here, we show that these puzzling observations are predicted if the receptor distribution in the olfactory epithelium is organized to present a maximally-informative picture of the odor environment. Specifically, we take the receptor-odorant affinities as given (unlike previous work (Keller and Vosshall, 2007; McBride et al., 2014; Zwicker et al., 2016; Krishnamurthy et al., 2017)), and propose a model for the quantitative distribution of olfactory sensory neurons by receptor type. The model predicts that in a noisy odor environment: (a) the distribution of receptor types will be highly non-uniform, but reproducible given fixed receptor affinities and odor statistics, and (b) an adapting receptor neuron repertoire should reproducibly reflect changes in the olfactory environment; in a sense it should become what it smells. Precisely such findings are reported in experiments (Schwob et al., 1992; Santoro and Dulac, 2012; Zhao et al., 2013; Dias and Ressler, 2014; Cadiou et al., 2014; Ibarra-Soria et al., 2017).

Because of the combinatorial nature of the olfactory code (Malnic et al., 1999; Stopfer et al., 2003; Stevens, 2015; Zhang and Sharpee, 2016; Zwicker et al., 2016; Krishnamurthy et al., 2017) receptor neuron responses are highly correlated. In the absence of such correlations, efficient coding predicts that output power will be equalized across all channels if transmission limitations dominate (Srinivasan et al., 1982; Olshausen and Field, 1996; Hermundstad et al., 2014), or that most resources will be devoted to receptors whose responses are most variable if input noise dominates (van Hateren, 1992a; Hermundstad et al., 2014). Here, we show that the optimal solution is very different when the system of sensors is highly correlated: the adaptive change in the abundance of a particular receptor type depends critically on the global context of the correlated responses of all the receptor types in the population—we refer to this as *context-dependent adaptation.*

In olfaction, sensor correlations are inevitable because the same odorant binds to many different receptors, and because odors in the environment are typically composed of many different molecules, leading to correlations between the concentrations with which these odorants are encountered. Furthermore, there is no way for neural circuitry to remove these correlations in the sensory epithelium because the candidate lateral inhibition occurs downstream, in the olfactory bulb. The outcome is that, for an adapting receptor neuron population, our model predicts that increased activation of a given receptor type may lead to *more, fewer or unchanged* numbers of the receptor, but that this apparently sporadic effect will actually be reproducible between replicates. This counter-intuitive prediction matches experimental observations (Santoro and Dulac, 2012; Zhao et al., 2013; Cadiou et al., 2014; Ibarra-Soria et al., 2017).

Olfactory response model

In vertebrates, axons from olfactory neurons converge in the olfactory bulb on compact structures called glomeruli, where they form synapses with dendrites of downstream neurons (Hildebrand and Shepherd, 1997); see Figure 1a. To good approximation, each glomerulus receives axons from only one type of OSN, and all OSNs expressing the same receptor type converge onto a small number of glomeruli, on average about 2 in mice to about 16 in humans (Maresh et al., 2008). Similar architectures can be found in insects (Vosshall et al., 2000).

The anatomy shows that in insects and vertebrates, olfactory information that is passed to the brain can be summarized by activity in the glomeruli. We will treat this activity in a firing-rate approximation, ignoring the timing of individual spikes. There is evidence that in mammals and in insects timing can be important for odor discrimination (Resulaj and Rinberg, 2015; DasGupta and Waddell, 2008; Wehr and Laurent, 1996; Huston et al., 2015). This could be incorporated into our model by using spike timing instead of the average firing rate as a measure of receptor activity, but we do not do so here. We will take all neurons of a given type to converge onto a single glomerulus (Figure 1a). If the receptor neuron output was split over multiple glomeruli our model would still make the same predictions for the total number of OSNs of each type. This is because the specific way in which these are partitioned into several glomeruli has no effect on the information transfer (see Supplementary Information).

A challenge specific to the study of the olfactory system as compared to other senses is the limited knowledge we have of the space of odors. It is difficult to identify common features shared by odorants that activate a given receptor type (Rossiter, 1996; Malnic et al., 1999), while attempts at defining a notion of distance in olfactory space have had only partial success (Snitz et al., 2013), as have attempts to find reduced-dimensionality representations of odor space (Zarzo and Stanton, 2006; Koulakov et al., 2011). In this work, we simply model the olfactory environment as a vector $\mathbf{c} = \{c_1, \ldots, c_N\}$ of concentrations, where c_i is the concentration of odorant i in the environment (Figure 1). In fact, our analysis does not depend in any way on this interpretation—it could instead represent a different abstraction, such as concentrations of classes of molecules clustered based on common chemical traits, or abstract coordinates in a low-dimensional representation of olfactory space.

With this parametrization, the statistics of natural scenes can be summarized by the joint probability distribution $P(c_1, \ldots, c_N)$. This ignores temporal correlations in olfactory cues, an approximation that has been used successfully in similar studies of the visual system (Tkacik et al., 2010; Hermundstad et al., 2014). To construct a tractable model of the relation between natural odor statistics and olfactory receptor distributions, we model the probability distribution of the

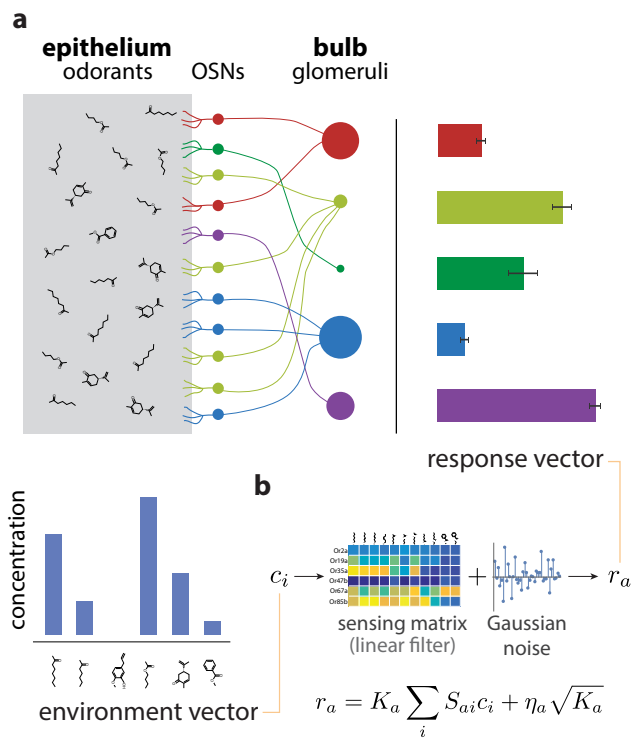

Figure 1: Sketch of the olfactory periphery as described in our model. **(a)** Sketch of vertebrate olfactory anatomy. In insects, the antennae and antennal lobes contain the OSNs and glomeruli, respectively. Different receptor types are represented by different colors. Glomerular responses (bar plot on top right) result from mixtures of odorants in the environment (bar plot on bottom left). The response noise, shown by black error bars, depends on the number of receptors of each type, illustrated in the figure by the size of the corresponding glomerulus. Glomeruli receiving input from a small number of OSNs have higher variability due to receptor noise (*e.g.,* OSN, glomerulus, and activity bar in dark green), while those receiving input from many OSNs have smaller variability. Response magnitudes depend also on the odorants present in the medium and the affinity profile of the receptors (*e.g.,* blue bar is smaller than green bar despite blue glomerulus being larger). **(b)** We approximate glomerular responses using a linear model based on a "sensing matrix" S, perturbed by Gaussian noise η_a. K_a are the multiplicities of each receptor type.

environment vector as a multivariate Gaussian with mean $\mathbf{c}_0$ and covariance matrix Γ,

$$\text{environment } P(\mathbf{c}) \sim \mathcal{N}(\mathbf{c}_0, \Gamma)\,. \tag{1}$$

We are interested in ensembles of odorants that are encountered at meaningful concentrations in a given environment. This number, N, though large, will be much smaller than the total number of possible volatile molecules. Our quantitative analyses will be based on experimental receptor affinity data measured using panels of 110 odorants in fly (Hallem and Carlson, 2006) and 63 in mammals (Saito et al., 2009).

Olfactory sensory neurons can show significant nonlinearities in their responses to odors. However, the mutual information between odor inputs and glomerular responses is invariant to such nonlinearities so long as (a) the dominant noise source is in the receptors, and (b) responses are above threshold and below saturation (see Discussion). Thus, we choose an operating point that satisfies these assumptions, and linearize around it to arrive at the glomerual response model as a sum of the responses from all the neurons that project to it, with additive noise:

$$r_a = K_a \sum_i S_{ai} c_i + \eta_a \sqrt{K_a}\,, \tag{2}$$

where r_a is the response of the glomerulus indexed by a, S_{ai} is the expected response of a sensory neuron expressing receptor type a to a unit concentration of odorant i, and K_a is the number of neurons of type a. The second term describes noise, with η_a, the noise for a single OSN, modeled as a Gaussian. Responses are normalized by the single neuron noise standard deviation; so η_a are drawn from independent standard normal distributions. In this description, changes in the number of receptor molecules per neuron have the same effect as changes in the number of olfactory neurons of a given type.

Information maximization

We quantify the information that responses $\mathbf{r}$ contain about the environment vector $\mathbf{c}$ as the mutual information $I(\mathbf{r}, \mathbf{c})$:

$$I(\mathbf{r}, \mathbf{c}) = \int d^M r d^N c\, P(\mathbf{r}, \mathbf{c}) \cdot \log \left[\frac{P(\mathbf{r}|\mathbf{c})}{P(\mathbf{r})} \right]\,, \tag{3}$$

where $P(\mathbf{r}, \mathbf{c})$ is the joint probability distribution over response and concentration vectors, $P(\mathbf{r}|\mathbf{c})$ is the distribution of responses conditioned on the environment, and $P(\mathbf{r})$ is the marginal distribution of the responses alone. Given our assumptions, all of these distributions are Gaussian, and the integral can be evaluated analytically (see Supplementary Information). The result is

$$I(\mathbf{r}, \mathbf{c}) = \frac{1}{2} \operatorname{Tr} \log(\mathbb{I} + \mathbb{K} Q)\,, \tag{4}$$

where the *overlap matrix* Q is related to the covariance matrix Γ of odorant concentrations (from eq. (1)),

$$Q = S \Gamma S^T\,, \tag{5}$$

and $\mathbb{K}$ is a diagonal matrix of receptor abundances K_a,

$$\mathbb{K} = \operatorname{diag}\big(K_1, K_2, \ldots, K_M\big)\,. \tag{6}$$

In the absence of noise, the overlap matrix Q equals the covariance matrix of receptor responses averaged over the odor ensemble. The quantity $\mathbb{K}Q$ thus behaves as a signal-to-noise ratio (SNR), so that eq. (4) is essentially a generalization to multiple, correlated channels of the standard result for a single Gaussian channel, $I = \frac{1}{2}\log(1 + \mathrm{SNR}^2)$ (Shannon, 1948; van Hateren, 1992b,a).

The receptor numbers K_a are constrained by the total number of neurons in the olfactory epithelium. Thus, to find the optimal distribution of receptor types, we maximize $I(\mathbf{r}, \mathbf{c})$ with respect to $\{K_a\}$, subject to the constraints that: (1) the total number of receptor neurons is fixed ($\sum_a K_a = K_{\mathrm{tot}}$); and (2) all neuron numbers are non-negative. The optimization can be performed

analytically using the Karush-Kuhn-Tucker (KKT) conditions (Boyd and Vandenberghe, 2004) (see Supplementary Information), but in practice it is more convenient to use numerical optimization. Below we analyze how the optimal distribution of receptor types depends on receptor affinities, odor statistics, and the size of the olfactory epithelium.

All receptors are equally represented in large OSN populations

In our model, receptor noise is reduced by averaging over the responses from many sensory neurons. As the number of neurons increases, $K_{\text{tot}} \to \infty$, the signal-to-noise ratio (SNR) becomes very large (see eq. (2)). When this happens, the optimization with respect to receptor numbers K_a can be solved analytically (see Supplementary Information), and we find that the optimal receptor distribution is given by

$$K_a = \frac{K_{\text{tot}}}{M} - (A_{aa} - \bar{A}) + \mathcal{O}(A^2/K^2)\,, \tag{7}$$

where A is the inverse of the overlap matrix defined in eq. (5), $A = Q^{-1}$, and $\bar{A} = \sum A_{aa}/M$ is the average diagonal element of this matrix. In other words, the receptor distribution is essentially uniform, with each receptor type being expressed in a roughly equal fraction of the total population of sensory neurons, with small differences related to the diagonal elements of the inverse overlap matrix A (see Figure 2a). It turns out also that the information maximum in this regime is very shallow. This is because only a change in receptor numbers of order K_{tot}/M can have a significant effect on the noise level for the activity of each glomerulus. Put another way, when the receptor numbers K_a are very large, the responses are effectively noiseless, and the number of receptors of each type has little effect on the reliability of the responses. The approximation in eq. (7) holds as long as the receptor abundances K_a are much larger than the elements of the inverse overlap matrix A, and breaks down otherwise (see the points on the right in Figure 2f).

Smaller OSN populations have less diverse receptors

When the number of neurons is very small, receptor noise can overwhelm the response to the environment. In this case, we find that the best strategy is to focus all the available neurons on a single receptor type, thus reducing noise as much as possible (Figure 2b). The receptor type that yields the highest contribution to the information turns out to be the one whose response is most variable in natural scenes (that is, the one that corresponds to the largest value of Q_{aa}; see Supplementary Information for a derivation). This is reminiscent of a result in vision where the variance of a stimulus predicted its perceptual salience (Hermundstad et al., 2014). As the total number of neurons increases, the added benefit from lowering the noise for a single receptor type diminishes, and at some critical value it becomes more advantageous in terms of maximizing information to start populating a second receptor type (Figure 2b). Thus, in an intermediate SNR range, where noise is significant but does not overwhelm the olfactory signal our model predicts a highly non-uniform distribution of receptor types. Indeed, an inhomogeneous distribution of this kind is seen in mammals (Ibarra-Soria et al., 2017). This is consistent with the idea that living systems conserve resources and thus would set the number of OSNs (and, thus, the SNR) close to the minimum necessary.

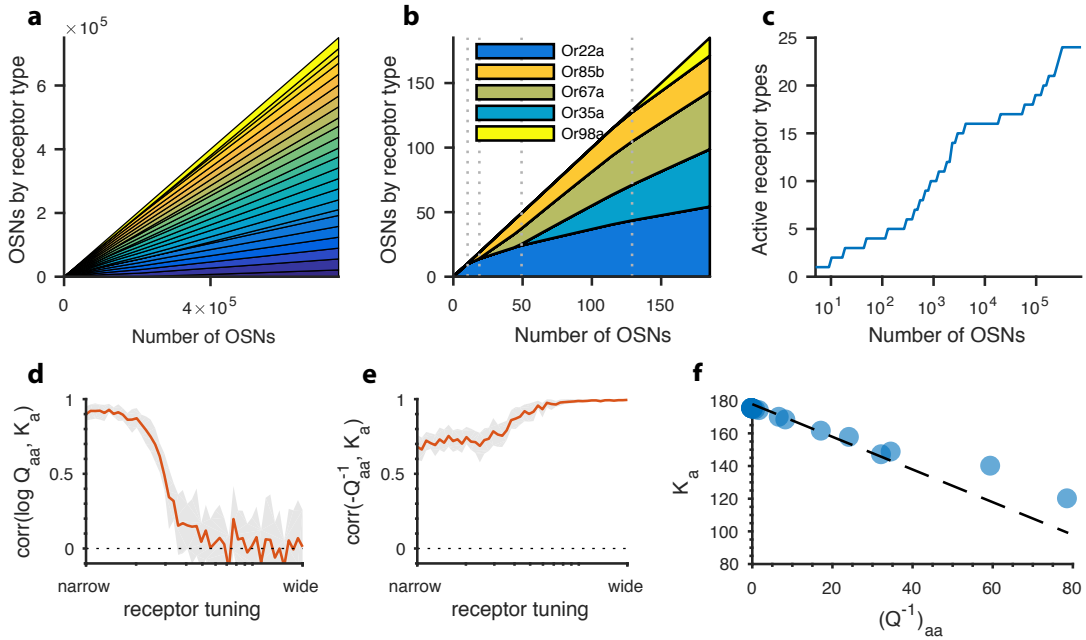

Figure 2: Building an intuition for the results from our model. **(a)** When the total number of neurons, K_{tot}, is large, the optimal distribution of receptors is approximately uniform, with each receptor type taking up an equal fraction of the total (represented here by strips of different colors). **(b)** When the number of neurons K_{tot} is low, only a small number of receptor types are expressed when information is maximized. **(c)** New receptor types become expressed in a series of step transitions as the total number of neurons increases. In panels **a**–**c**, results were obtained using a sensing matrix based on measurements in the fly (Hallem and Carlson, 2006) and environmental odor statistics following a random correlation matrix (see Supplementary Information for details). However, the qualitative aspects are generic. **(d)** Correlation between the abundance of a given receptor type, K_a, and the logarithm of the variance with which it is activated in olfactory scenes, $\log Q_{aa}$, shown here as a function of the tuning of the receptors. For every position along the x-axis, sensing matrices with a fixed receptor tuning width were generated from a random ensemble. Roughly-speaking, the tuning width on the x-axis indicates what fraction of all odorants elicit a strong response for the receptors; in the figure, this ranges from 0.01 to 0.2. See Supplementary Information for details. When each receptor responds strongly to only a small number of odorants, response variance is a good predictor of abundance, while this is no longer true for wide tuning. **(e)** Receptor abundances correlate well with the diagonal elements of the inverse overlap matrix, $(Q^{-1})_{aa}$, for all tuning widths, with somewhat lower correlations at narrow tuning. In **d** and **e**, the red line is the mean obtained from 24 simulations, each performed using a different sensing matrix, and the light gray area shows the interval between the 20th and 80th percentiles of results. **(f)** Example showing the dependence between receptor abundances and the diagonal elements of the inverse overlap matrix in a simulation using a wide-tuning sensing matrix and an intermediate SNR. The dashed line corresponds to the approximation from eq. (7).

Receptor diversity grows with OSN population size

More generally, our model predicts that the number of receptor types that are expressed should increase monotonically with the total number of sensory neurons, in a series of step transitions (see Figure 2c). This provides an interesting prediction that could be tested by looking at the relation between the size of the olfactory epithelium and the number of functional receptor genes in various species. A caveat here is that we are assuming the sensing matrix S and environmental statistics Γ stay the same while varying only the total number of neurons K_{tot}. This restricts an empirical test of this prediction to groups of closely-related species.

Receptor abundances are highly context-dependent

By maximizing the mutual information in eq. (4) while keeping the total number of receptors $K_{\text{tot}} = \sum_a K_a$ constant, we can predict the optimal receptor distribution K_a given the sensing matrix S and the statistics of odors. The results reveal a surprise: optimal receptor abundances sometimes increase and sometimes decrease upon increased exposure to ligands. In fact, a puzzling pattern of this kind has been reported in recent experiments (Santoro and Dulac, 2012; Zhao et al., 2013; Cadiou et al., 2014; Ibarra-Soria et al., 2017). We sought an intuitive way to understand this result from our model.

A simple observation is that the average concentration vector $\mathbf{c}_0$ has no impact on the optimal distribution. This is because it corresponds to odors that are always present and thus offer no new information about the environment. This observation is consistent with experiment (Ibarra-Soria et al., 2017). Thus, environmental statistics affect the optimal receptor distribution only through the covariance matrix Γ.

It is intuitively clear that, at least in the limit in which receptor responses are uncorrelated, receptors whose activations fluctuate extensively in response to natural olfactory scenes provide the brain with a lot of information about the odor environment. In contrast, receptors that are almost silent or are constantly active at about the same rate are not very informative. It thus seems advantageous to increase the number of neurons expressing receptors with large response variance, and to not focus many resources on the others (Hermundstad et al., 2014). In terms of our model, the variance of glomerular responses is given (in the absence of noise) by diagonal elements of the overlap matrix Q defined in eq. (5); our intuition dictates that the number of receptors of type a should grow with the variance corresponding to that receptor type, $K_a \sim Q_{aa}$.

Even when there are correlations between receptor responses, the intuition above applies in the low SNR regime, when only one receptor type is active. As we saw in the previous section, in that case, the receptor type that should be active to maximize information is indeed the one with the largest variance Q_{aa}. The intuition also holds when the sensing matrix is narrowly-tuned: if each receptor type responds to only a small number of odorants, the abundances of OSNs of each type should correlate well with the amount of variability that the corresponding receptors experience (narrow-tuning side of Figure 2d). Thus in all these cases, the abundance of a receptor type is correlated to the variability of its responses in the environment, a result that coincides with conventional intuition.

The biological setting, however, is better described in our model by a regime with widely-tuned sensing matrices (Hallem and Carlson, 2006), and an intermediate SNR level in which noise is important, but does not dominate the responses of most receptors. To see how tuning width affects results from the model, we generated sensing matrices with varying tuning width by changing

the number of odorants that exhibit strong responses for each receptor (detailed Methods in Supplementary Information). We found that as each receptor type starts responding to more and more odorants, the *correlation structure* of the receptor responses becomes important in determining the optimal receptor distribution, and the intuition based on only the response variances no longer holds (wide-tuning side of Figure 2d). In other words the optimal abundance of a receptor type depends not just on its activity level, but also on the correlated activity levels of all the other receptor types.

One way to understand this context-dependence is to note that for intermediate SNR the optimal receptor distribution is anti-correlated with the diagonal elements of the *inverse* of the overlap matrix, $A = Q^{-1}$ (Figure 2e-f). This is an extension to intermediate SNR of the result that we proved analytically for high SNR in eq. (7). Because of the matrix inversion, the optimal distribution in these regimes is affected by the full covariance structure of the receptor responses. This leads to a complex context-dependence in the optimal abundance of receptor types. The appearance of the inverse overlap matrix Q^{-1} may seem surprising. In Supplementary Information we show that this occurs because receptors that have a high $(Q^{-1})_{aa}$ either do not provide much olfactory information because their responses do not fluctuate much; or they provide information that is largely redundant given all the others. Either way, they should therefore not be very abundant in the optimal distribution. In contrast, receptors with low $(Q^{-1})_{aa}$ contain a lot of independent olfactory information, and so they are predicted to be abundant.

Environmental changes lead to complex patterns of receptor abundance changes

To get an intuition for the effects of changes in odor statistics on the optimal receptor repertoire, we used a sensing matrix based on measurements in the fly (Hallem and Carlson, 2006), and compared the predicted receptor distributions in two different environments, at two different noise levels (or, equivalently, two different values for the total number of OSNs K_{tot}); see Figure 3.

We started with an odor environment eq. (1) with a random covariance matrix (see Figure 3a for an example; see Supplementary Information for details). From this base, we generated two different environments by adding a large variance to 10 odorants in environment 1, and to 10 different odorants in environment 2 (Figure 3b).

Our results show that, when the number of olfactory sensory neurons K_{tot} is large, and thus the signal-to-noise ratio is high, the change in odor statistics has little effect on the distribution of receptors (Figure 3c). This is because at high SNR, the distribution is essentially uniform regardless of environment, as explained earlier. When the number of neurons is smaller (or, equivalently, the signal to noise ratio is in a low or intermediate regime), the change in environment has a significant effect on the receptor distribution, with some receptor types becoming more abundant, others becoming less abundant, and yet others not changing much (see Figure 3d). This mimics the kinds of complex effects seen in experiments in mammals (Schwob et al., 1992; Santoro and Dulac, 2012; Zhao et al., 2013; Dias and Ressler, 2014; Cadiou et al., 2014; Ibarra-Soria et al., 2017).

Strikingly, and consistently with the findings in (Schwob et al., 1992; Santoro and Dulac, 2012; Zhao et al., 2013; Dias and Ressler, 2014; Cadiou et al., 2014; Ibarra-Soria et al., 2017), whether a certain receptor abundance goes up or down as a result of a given change in environment is hard to guess, as it is a global effect that depends on how the change affects the activation of all receptor types, as well as the correlations between these activations.

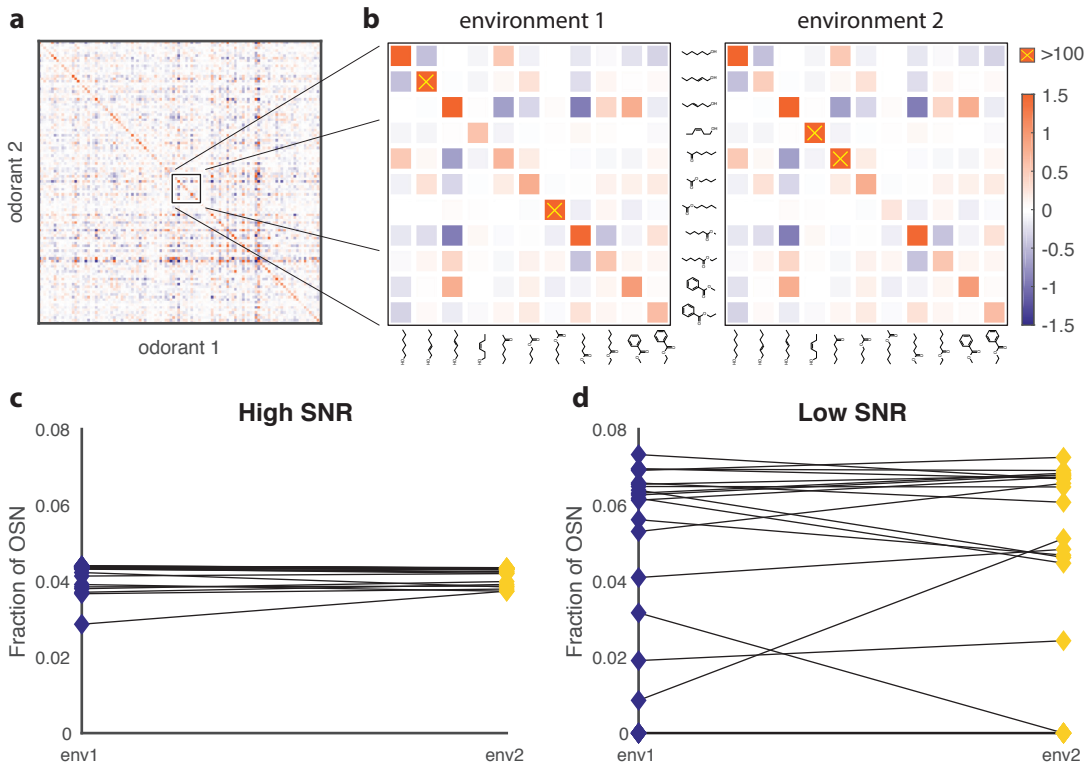

Figure 3: Effect of changing environment on the optimal receptor distribution in our model. **(a)** An example of an environment covariance matrix used in our model. We use an algorithm that generates random covariance matrices with a tunable amount of cross-correlation (see Supplementary Information for details). The variances are drawn from a lognormal distribution. **(b)** Close-ups showing some of the differences between the two environments used to generate the results from **c** and **d**. The two different covariance matrices are obtained by starting with the matrix from **a** and adding a large amount of variance to two different sets of 10 odorants (out of 110). The altered odorants are identified by yellow crosses; their corresponding variances go above the color scale on the plots by more than 60 times. **(c)** Change in receptor distribution when going from environment 1 to environment 2, in conditions where the total number of receptor neurons K_{tot} is large (the SNR is high). The blue diamonds on the left correspond to the optimal OSN fractions per receptor type in the first environment, while the yellow diamonds on the right correspond to the second environment. In this high-SNR regime, the effect of the environment is small, because in both environments the optimal receptor distribution is close to uniform. **(d)** When the total number of neurons K_{tot} is small (the SNR is low), changing the environment can have a dramatic effect on optimal receptor abundances, with some receptors that are almost vanishing in one setting becoming highly abundant in the other, and *vice versa*.

Changing odor identities has a larger effect on receptor distributions than changing concentrations

In the comparison above, the two environment covariance matrices differed in a small number of positions by a large amount. In contrast, Figure 4b shows what happens if we instead compare

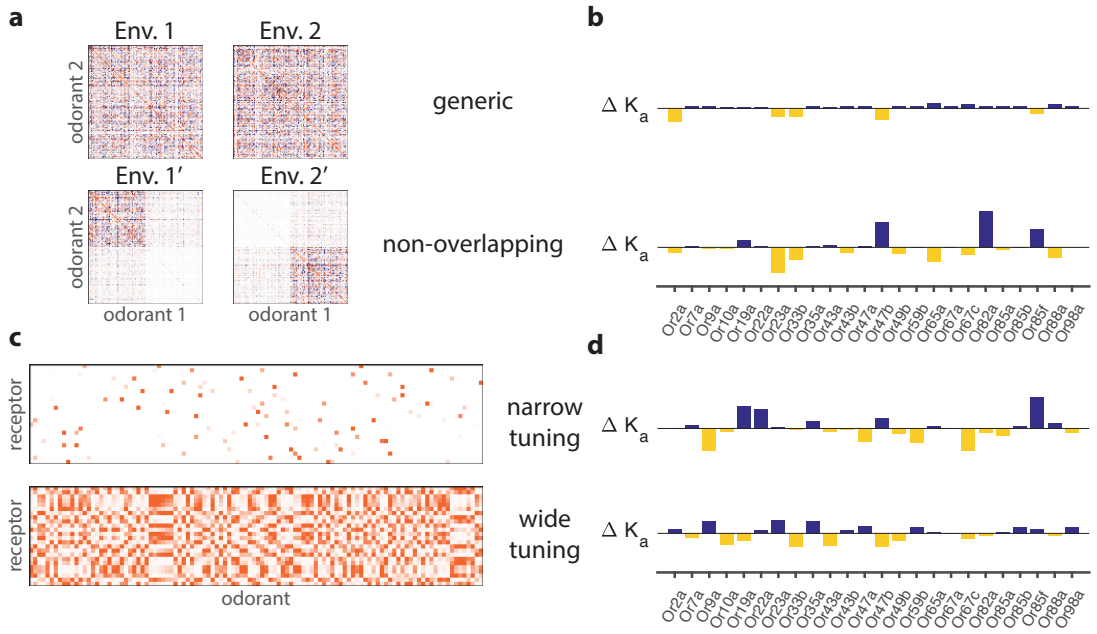

Figure 4: The effect of a change in environmental statistics on the optimal receptor distribution as a function of overlap in the odor content of the two environments, and the tuning properties of the olfactory receptors. **(a)** Random environment covariance matrices used in our simulations (red is positive [co-]variance, blue is negative, white is zero). The environments on the top span a similar set of odors, while those on the bottom contain largely non-overlapping sets of odors. **(b)** The change in receptor distribution tends to be small when both environments span a similar set of odors, even when the detailed statistics are very different (top). The change is much larger when the two environments contain different odors (bottom). The results in **a** and **b** are based on receptor affinity data from the fly (Hallem and Carlson, 2006) **(c)** Sensing matrices we used in our simulations. On top, a sensing matrix with narrowly-tuned receptors, which respond to small numbers of odorants (tuning parameter of 0.05—see Supplementary Information). On the bottom, a sensing matrix with broadly-tuned receptors (tuning parameter of 0.8—see Supplementary Information). **(d)** Narrowly-tuned receptors result in optimal receptor distributions that are more sensitive to changes in environment (top). Broadly-tuned receptors tend to average out differences in environmental statistics of odors (bottom).

environments with two different randomly-generated covariance matrices, each generated in the same way as the background environment in Figure 3a. The resulting covariance matrices (Figure 4a, top) are very different in detail (the correlation coefficient between their entries is close to zero), although they look similar by eye. Nevertheless, the corresponding change in receptor distribution is very small, with just a few receptor types experiencing larger changes in abundance (Figure 4b, top).

If instead we engineer two environments that are almost non-overlapping, meaning that each odorant is either common in environment 1, or in environment 2, but not in both (Figure 4a, bottom), the changes in receptor abundances become much larger, with some receptors going from highly abundant to vanishing from the population, while others going in the opposite direction, from not

being expressed at all, to high abundance (Figure 4b, bottom). This shows that the particular way in which the environment changes, and not only the magnitude of the change, can alter the effect on the receptor distribution. In biological terms, we would indeed expect animals that experience very different kinds of odors to have more striking differences in their receptor repertoires than those that merely experience the same odors with different frequencies. Our results quantify the expected difference.

The magnitude of the effect of environmental changes on the optimal olfactory receptor distribution is partly controlled by the tuning of the olfactory receptors (Figure 4c). If receptors are narrowly-tuned, with each type responding to a small number of odorants, changes in environment tend to have more drastic effects on the receptor distribution than when the receptors are broadly-tuned (Figure 4d), an effect that could be experimentally tested.

Model predictions qualitatively match experiments

Our study opens the exciting possibility of a causal test of the hypothesis of efficient coding in sensory systems, where a perturbation in the odor environment could lead to predictable adaptations of the olfactory receptor distribution during the lifetime of an individual. This does not happen in insects, but it can happen in mammals, since their receptor neurons regularly undergo apoptosis and are replaced.

A recent study demonstrated that reproducible changes in olfactory receptor distributions of the sort that we predict can occur in mice (Ibarra-Soria et al., 2017). Specifically, Ibarra-Soria et al. (2017) raised two groups of mice in similar conditions, exposing one group to a mixture of four odorants (acetophenone, eugenol, heptanal, and R-carvone) either continuously or intermittently (by adding the mixture to their water supply). Continuous exposure to the odorants had no effect on the receptor distribution, in agreement with the predictions of our model, in which the average concentration vector $\mathbf{c}_0$ drops out of the mutual information calculations. In contrast, intermittent exposure did lead to systematic changes in the receptor distribution (see Figure 5a).

We used our model to run an experiment similar to that of Ibarra-Soria et al. (2017) *in silico*. Using a sensing matrix based on odor response curves for mouse and human receptors (Saito et al., 2009), we calculated the predicted change in receptor abundances between two different environments with random covariance matrices. The results (see Figure 5b) show that most receptor abundances do not change much, especially for those receptors that were very abundant to start with; there is more change in the middle of the abundance range; while the abundances of rare receptors change significantly, but are highly sensitive to small perturbations in the environment. The sensitivity to perturbations was estimated by running the simulation 24 times, each time modifying the covariance matrices for the initial and final environments. This was done by adding a small amount of Gaussian random noise to the square roots of these covariance matrices (see Supplementary Information).

The simulation results qualitatively match the experimental results (see Figure 5a), where we see the same pattern of the largest reproducible changes occurring for receptors with intermediate abundances. This comparison could be made quantitative by using the same perturbation in our simulations as that used in the experiments from (Ibarra-Soria et al., 2017). Doing this in detail requires sensing data for all the mouse receptor types responding to all four odorants used in the experiments. Surveys of this kind can be anticipated in the future. Likewise we can expect more detailed information about natural environments which will also inform the quantitative predictions of our model.

First steps towards a dynamical model in mammals

We have explored the structure of olfactory receptor distributions that code odors efficiently, *i.e.,* are adapted to maximize the amount of information that the brain gets about odors. The full solution to the optimization problem depends in a complicated nonlinear way on the receptor affinities S and covariance of odorant concentrations Γ. The distribution of olfactory receptors in the mammalian epithelium, however, must arise dynamically, from the pattern of apoptosis and neurogenesis (Calof et al., 1996). In the efficient coding paradigm that we propose, the receptor distribution is intimately related to the statistics of natural odors, so that the life cycle of neurons in a dynamical model implementation would have to depend on olfactory experience. And indeed, such modulation of OSN lifetime by exposure to odors has been observed experimentally (Santoro and Dulac, 2012; Zhao et al., 2013; Cadiou et al., 2014) and could, for example, be mediated by feedback from the bulb (Schwob et al., 1992).

To obtain a dynamical version of our model, we started with a gradient ascent algorithm and modified it slightly to impose the constraints that receptor numbers are non-negative, $K_a \geq 0$, and their sum $K_{\text{tot}} = \sum_a K_a$ is bounded (details in Supplementary Information). This gives

$$\frac{dK_a}{dt} = \alpha \left\{ K_a - \lambda K_a^2 - (R^{-1})_{aa} K_a^2 \right\} , \tag{8}$$

where α is a learning rate and R is the covariance matrix of glomerular responses,

$$R_{ab} = \langle r_a r_b \rangle - \langle r_a \rangle \langle r_b \rangle , \tag{9}$$

with the angle brackets denoting ensemble averaging over odors and averaging over receptor noise. In the absence of the experience-related term $(R^{-1})_{aa}$, the dynamics from eq. (8) would be simply logistic growth: the population of OSNs of type a would initially grow at a rate α, but would saturate when $K_a = 1/\lambda$ because of the population-dependent death rate λK_a. In other words, the quantity M/λ sets the asymptotic value for the total population of sensory neurons, $K_{\text{tot}} \to M/\lambda$, with M being the number of receptor types.

Because of the last term in eq. (8), the death rate in our model is influenced by olfactory experience in a receptor-dependent way. In contrast, the birth rate is not experience-dependent, and is the same for all OSN types. And indeed, in experiments, the odor environment is seen to have little effect on receptor choice, but does modulate the rate of apoptosis in the olfactory epithelium (Santoro and Dulac, 2012). Our results suggest that, if olfactory sensory neuron lifetimes are appropriately anti-correlated with the inverse response covariance matrix, then the receptor distribution in the epithelium can converge to achieve optimal information transfer to the brain.

The elements of the response covariance matrix R_{ab} could be estimated by taking temporal averages of co-occurring glomerular activations. This computation could exploit the lateral connections between glomeruli (Mori et al., 1999). Performing the inverse necessary for our model is more intricate, but this could be done at the level of the bulb and fed back to the epithelium through mechanisms that have been observed in experiments (Schwob et al., 1992). We leave development of these ideas for future work.

Within our model, Figure 5c shows example convergence curves when starting from a random initial distribution. The sensing matrix used here is based on mammalian data (Saito et al., 2009) and the environment covariance matrix is generated using the random procedure mentioned earlier (and described in the Supplementary Information). We see that some receptor types take much longer than others to converge (the time axis is logarithmic, which helps visualize the whole range of

convergence behaviors). Roughly speaking, convergence is slower when the final receptor abundance is small, which is related to the fact that the rate of change dK_a/dt in eq. (8) vanishes in the limit $K_a \to 0$.

In Figure 5d, we show convergence to the same final state, but this time starting from a distribution that is not random, but was optimized for a different environment. The initial and final environments are the same as those used in the previous section to compare the simulations to experimental findings, Figure 5b. Interestingly, many receptor types actually take longer to converge in this case compared to the random starting point, showing that getting trapped in local optima is a potential danger. This can be alleviated by adding a small amount of stochasticity to the dynamics, which in realistic situations would enter naturally since the response covariance matrix R would have to be estimated based on stochastic odor encounters and noisy receptor readings. In fact, in Figure 5d, we needed to add a small amount of noise (corresponding to $\pm 0.05 K_{\text{tot}}$) to the initial distribution to improve convergence and avoid getting trapped.

Discussion

We built a model for the distribution of receptor types in the olfactory epithelium that is based on efficient coding, and assumes that the abundances of different receptor types are adapted to the statistics of natural odors in a way that maximizes the amount of information conveyed to the brain by glomerular responses. This model predicts a non-uniform distribution of receptor types in the olfactory epithelium, as well as reproducible changes in the receptor distribution after perturbations to the odor environment. In contrast to other applications of efficient coding, our model operates in a regime in which there are significant correlations between sensors because the adaptation of receptor abundances occurs upstream of the brain circuitry that can decorrelate olfactory responses. In this regime, receptor abundances depend on the full correlation structure of the inputs, leading to predictions that are context-dependent in the sense that whether the abundance of a specific receptor goes up or down due to a shift in the environment depends on the global context of the responses of all the other receptors. All of these striking phenomena have been observed in recent experiments.

In our framework, the sensitivity of the receptor distribution to changes in odor statistics is affected by the tuning of the olfactory receptors, with narrowly-tuned receptors being more readily affected by such changes than broadly-tuned ones. The model also predicts that environments that differ in the identity of the odors that are present will lead to larger differences in optimal receptor distribution than environments that differ only in the statistics with which these odors are encountered. Another prediction is that there is a monotonic relationship between the number of receptor types found in the epithelium and the total number of olfactory sensory neurons. All of these predictions can be tested in future experiments.

OSN responses can manifest complex, nonlinear responses to odor mixtures. In fact, such nonlinearities do not significantly affect the results from our model provided the responses do not saturate, because mutual information between odor inputs and receptor neuron responses is unaffected by such transformations. Specifically, our results would not change if the concentration vector was first passed through an invertible nonlinearity, then mixed according to the sensing matrix, scaled according to the receptor numbers and perturbed by noise, and finally passed through another invertible nonlinearity. These transformations could, however, make it harder to decode the processed information. This means that the fundamental assumption of our model is not that OSN responses are linear, but rather that the dominant source of noise is from the receptors, and that

downstream processing has the precision to usefully process all the information transcribed by the receptors.[1] Thus, generalizing our model to include nonlinear responses is effectively equivalent to including noise beyond the receptor level.

Other assumptions of our model are easily relaxed. For example, the distribution of odorants could be modeled using a Gaussian mixture, rather than the normal distribution used in this paper to enable analytic calculations. Each Gaussian in the mixture would model a different odor object in the environment, more closely approximating the sparse nature of olfactory scenes (Krishnamurthy et al., 2017). Likewise, we could extend the model to include some notion of the value of detecting different odorants, since mutual information, the quantity we maximized, may not necessarily be a good measure of the quality of the olfactory representation (Rivoire and Leibler, 2011). In general, understanding the role of value in shaping neural circuits is an important experimental and theoretical problem.

Our framework suggests several directions for future experimental work that would test our model and its extensions. More complete surveys of olfactory receptor responses to larger panels of odorants in more organisms would help to fix the structure of odor-receptor interactions that is necessary for our model. More high-throughput measurements of the distribution of receptor types in the olfactory epithelium, as in (Ibarra-Soria et al., 2017), would enable precise tests of the predictions. Direct measurements of the statistics of natural odors would improve the accuracy of quantitative predictions from our model. Such measurements are difficult, so imaging studies focusing on glomeruli in behaving animals could provide an alternate way to obtain this data. Conversely, given measurements of olfactory receptor distributions, the predictions of our theory could be inverted to give hypotheses for natural odor statistics.

One exciting possibility suggested by our model is a way to perform a first causal test of the efficient coding hypothesis for sensory coding. Given sufficiently-detailed information regarding receptor affinities and natural odor statistics, experiments could be designed that perturb the environment in specified ways, and then measure the change in olfactory receptor distributions. Comparing the results to the changes predicted by our theory would provide a strong test of efficient coding by early sensory systems in the brain.

Materials and methods

Software and data

The code and data that we used to generate all the results and figures in the paper is available on GitHub, at `https://github.com/ttesileanu/OlfactoryReceptorDistribution`.

Acknowledgments

We would like to thank Joel Mainland and David Zwicker for helpful discussions, and Elissa Hallem, Joel Mainland, and Darren Logan for olfactory receptor affinity data. During the completion of this project, VB was supported by Simons Foundation Mathematical Modeling in Living Systems grant 400425 and by the Aspen Center for Physics NSF grant PHY-160761. TT was supported by the Swartz Foundation. This work was also supported by NSF grant PHY-1734030.

[1] We thank David Zwicker for illuminating discussions regarding this point.

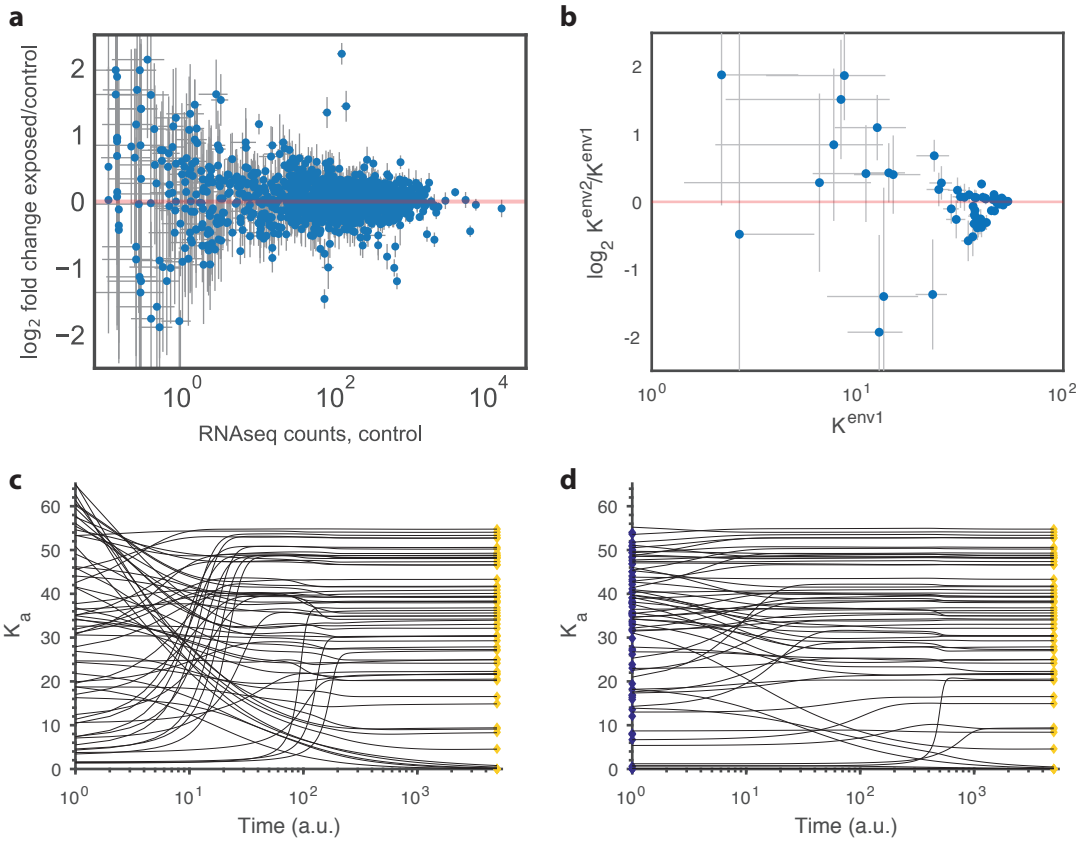

Figure 5: Qualitative comparison between experiment and theory regarding the changes in receptor distribution that occur with a change in environment; and an example of convergence in our dynamical model. **(a)** Reproduced using the raw data from (Ibarra-Soria et al., 2017), this shows the experimental data for the log-ratio between the receptor abundances in the mouse epithelium in the test environment (where four odorants were added to the water supply) and those in the control environment, plotted against the values in the control conditions (on a log scale). The error bars show standard deviation across six individuals. Compared to Figure 5B in (Ibarra-Soria et al., 2017), this plot does not use a Bayesian estimation technique that shrinks ratios of abundances of rare receptors towards 1 (personal communication with Professor Darren Logan, June 2017). **(b)** A similar plot produced in our model using mouse and human receptor response curves (Saito et al., 2009). The error bars show the range of variation found in the optimal receptor distribution when slightly perturbing the initial and final environments (see the text). The simulation includes 62 receptor types for which response curves were measured (Saito et al., 2009), compared to 1115 receptor types assayed in (Ibarra-Soria et al., 2017). **(c)** Example convergence curves in our dynamical model showing how the optimal receptor distribution (yellow diamonds) is reached from a random initial distribution of receptors. Note that the time axis is logarithmic. **(d)** Convergence curves when starting close to the optimal distribution from one environment (blue diamonds) but optimizing for another. A small, random deviation from the optimal receptor abundance in the initial environment was added to avoid the simulation getting trapped in a local optimum.

References

Atick, J. J. and Redlich, A. N. (1990). Towards a Theory of Early Visual Processing. *Neural Computation*, 2:308–320.

Barlow, H. B. (1961). Possible principles underlying the transformations of sensory messages. *Sensory Communication*, pages 217–234.

Boyd, S. and Vandenberghe, L. (2004). *Convex Optimization*. Cambridge University Press.

Buck, L. and Axel, R. (1991). A novel multigene family may encode odorant receptors: A molecular basis for odor recognition. *Cell*, 65(1):175–187.

Cadiou, H., Aoudé, I., Tazir, B., Molinas, A., Fenech, C., Meunier, N., and Grosmaitre, X. (2014). Postnatal Odorant Exposure Induces Peripheral Olfactory Plasticity at the Cellular Level. *Journal of Neuroscience*, 34(14):4857–4870.

Calof, A. L., Hagiwara, N., Holcomb, J. D., Mumm, J. S., and Shou, J. (1996). Neurogenesis and cell death in olfactory epithelium. *Journal of Neurobiology*, 30(1):67–81.

Chess, A., Simon, I., Cedar, H., and Axel, R. (1994). Allelic inactivation regulates olfactory receptor gene expression. *Cell*, 78(5):823–834.

DasGupta, S. and Waddell, S. (2008). Learned odor discrimination in Drosophila without distinct combinatorial maps in the antennal lobe. *Current Biology*, 18(21):1668–1674.

Dias, B. G. and Ressler, K. J. (2014). Parental olfactory experience influences behavior and neural structure in subsequent generations. *Nature neuroscience*, 17(1):89–96.

Fairhall, A. L., Lewen, G. D., and Bialek, W. (2001). Efficiency and ambiguity in an adaptive neural code. *Nature*, 412(August):787–792.

Garrigan, P., Ratliff, C. P., Klein, J. M., Sterling, P., Brainard, D. H., and Balasubramanian, V. (2010). Design of a trichromatic cone array. *PLoS Computational Biology*, 6(2):e1000677.

Hallem, E. A. and Carlson, J. R. (2006). Coding of odors by a receptor repertoire. *Cell*, 125(1):143–160.

Hermundstad, A. M., Briguglio, J. J., Conte, M. M., Victor, J. D., Balasubramanian, V., and Tkacik, G. (2014). Variance predicts salience in central sensory processing. *eLife*, 10.7554:e03722.

Hildebrand, J. G. and Shepherd, G. M. (1997). Mechanisms of olfactory discrimination: converging evidence for common principles across phyla. *Annual Review of Neuroscience*, 20:595–631.

Huston, S. J., Stopfer, M., Cassenaer, S., Aldworth, Z. N., and Laurent, G. (2015). Neural Encoding of Odors during Active Sampling and in Turbulent Plumes. *Neuron*, 88:1–16.

Ibarra-Soria, X., Nakahara, T. S., Lilue, J., Jiang, Y., Trimmer, C., Souza, M. A. A., Netto, P. H. M., Ikegami, K., Murphy, N. R., Kusma, M., Kirton, A., Saraiva, L. R., Keane, T. M., Matsunami, H., Mainland, J. D., Papes, F., and Logan, D. W. (2017). Variation in olfactory neuron repertoires is genetically controlled and environmentally modulated. *eLife*, 6:e21476.

Keller, A. and Vosshall, L. B. (2007). Influence of odorant receptor repertoire on odor perception in humans and fruit flies. *Proceedings of the National Academy of Sciences of the United States of America*, 104(13):5614–9.

Koulakov, A. A., Kolterman, B. E., Enikolopov, A. G., and Rinberg, D. (2011). In search of the structure of human olfactory space. *Frontiers in Systems Neuroscience*, 5(September):1–8.

Krishnamurthy, K., Hermundstad, A. M., Mora, T., Walczak, A. M., and Balasubramanian, V. (2017). Disorder and the neural representation of complex odors: smelling in the real world. *arXiv*.

Laughlin, S. (1981). A Simple Coding Procedure Enhances a Neuron's Information Capacity. *Z. Naturforsch.*, 36(c):910–912.

Lewandowski, D., Kurowicka, D., and Joe, H. (2009). Generating random correlation matrices based on vines and extended onion method. *Journal of Multivariate Analysis*, 100(9):1989–2001.

Lewicki, M. S. (2002). Efficient coding of natural sounds. *Nature neuroscience*, 5(4):356–363.

Malnic, B., Hirono, J., Sato, T., and Buck, L. B. (1999). Combinatorial receptor codes for odors. *Cell*, 96(5):713–23.

Maresh, A., Rodriguez Gil, D., Whitman, M. C., and Greer, C. A. (2008). Principles of glomerular organization in the human olfactory bulb - Implications for odor processing. *PLoS ONE*, 3(7).

McBride, C. S., Baier, F., Omondi, A. B., Spitzer, S. A., Lutomiah, J., Sang, R., Ignell, R., and Vosshall, L. B. (2014). Evolution of mosquito preference for humans linked to an odorant receptor. *Nature*, 515(7526):222–227.

Missbach, C., Dweck, H. K., Vogel, H., Vilcinskas, A., Stensmyr, M. C., Hansson, B. S., and Grosse-Wilde, E. (2014). Evolution of insect olfactory receptors. *eLife*, 2014(3):e02115.

Monti Graziadei, G. A. and Graziadei, P. P. C. (1979). Neurogenesis and neuron regeneration in the olfactory system of mammals. II. Degeneration and reconstitution of the olfactory sensory neurons after axotomy. *Journal of Neurocytology*, 8(2):197–213.

Mori, K., Nagao, H., and Yoshihara, Y. (1999). The olfactory bulb: Coding and processing of odor molecule information. *Science*, 286(5440):711–715.

Olshausen, B. A. and Field, D. J. (1996). Emergence of simple-cell receptive field properties by learning a sparse code for natural images. *Nature*, 381(June):607–609.

Palmer, S. E., Marre, O., Berry, M. J. I., and Bialek, W. (2015). Predictive information in a sensory population. *PNAS*, 112(22):6908–6913.

Ratliff, C. P., Borghuis, B. G., Kao, Y.-H., Sterling, P., and Balasubramanian, V. (2010). Retina is structured to process an excess of darkness in natural scenes. *PNAS*, 107(40):17368–17373.

Resulaj, A. and Rinberg, D. (2015). Novel Behavioral Paradigm Reveals Lower Temporal Limits on Mouse Olfactory Decisions. *Journal of Neuroscience*, 35(33):11667–11673.

Rivoire, O. and Leibler, S. (2011). The Value of Information for Populations in Varying Environments. *Journal of Statistical Physics*, 142:1124–1166.

Rospars, J.-P. and Chambille, I. (1989). *Identified Glomeruli in the Antennal Lobes of Insects: In Variance, Sexual Variation and Postembryonic Development*, pages 355–375. Springer US, Boston, MA.

Rossiter, K. J. (1996). Structure-odor relationships. *Chemical Reviews*, 96(8):3201–3240.

Saito, H., Chi, Q., Zhuang, H., Matsunami, H., and Mainland, J. D. (2009). Odor Coding by a Mammalian Receptor Repertoire. *Science Signaling*, 2(60):ra9.

Salisbury, J. M. and Palmer, S. E. (2016). Optimal Prediction in the Retina and Natural Motion Statistics. *Journal of Statistical Physics*, 162(5):1309–1323.

Santoro, S. W. and Dulac, C. (2012). The activity-dependent histone variant H2BE modulates the life span of olfactory neurons. *eLife*, 2012(1):1–32.

Schwob, J. E., Mieleszko Szumowski, K. E., and Stasky, A. A. (1992). Olfactory sensory neurons are trophically dependent on the olfactory bulb for their prolonged survival. *The Journal of Neuroscience*, 12(10):3896–3919.

Shannon, C. E. (1948). A mathematical theory of communication. *ACM SIGMOBILE Mobile Computing and Communications*, 27(July).

Simoncelli, E. P. and Olshausen, B. A. (2001). Natural image statistics and neural representation. *Annual Review of Neuroscience*, 24:1193–1216.

Snitz, K., Yablonka, A., Weiss, T., Frumin, I., Khan, R. M., and Sobel, N. (2013). Predicting Odor Perceptual Similarity from Odor Structure. *PLoS Computational Biology*, 9(9).

Srinivasan, M. V., Laughlin, S. B., and Dubs, A. (1982). Predictive Coding: A Fresh View of Inhibition in the Retina. *Proceedings of the Royal Society B: Biological Sciences*, 216(1205):427–459.

Stevens, C. F. (2015). What the fly's nose tells the fly's brain. *PNAS*, 112(30):9460–5.

Stopfer, M., Jayaraman, V., and Laurent, G. (2003). Intensity versus identity coding in an olfactory system. *Neuron*, 39(6):991–1004.

Tan, L., Li, Q., and Xie, X. S. (2015). Olfactory sensory neurons transiently express multiple olfactory receptors during development. *Molecular systems biology*, 11(12):844.

Tkacik, G., Prentice, J. S., Victor, J. D., and Balasubramanian, V. (2010). Local statistics in natural scenes predict the saliency of synthetic textures. *Proceedings of the National Academy of Sciences of the United States of America*, 107(42):18149–18154.

van Hateren, J. H. (1992a). A theory of maximizing sensory information. *Biological Cybernetics*, 68(1):23–29.

van Hateren, J. H. (1992b). Theoretical predictions of spatiotemporal receptive fields of fly LMCs, and experimental validation. *Journal of Comparative Physiology A*, 171:157–170.

Vosshall, L. B., Wong, A. M., and Axel, R. (2000). An olfactory sensory map in the fly brain. *Cell*, 102(2):147–159.

Wehr, M. and Laurent, G. (1996). Odour encoding by temporal sequences of firing in oscillating neural assemblies. *Nature*, 384(November):162–166.

Zarzo, M. and Stanton, D. T. (2006). Identification of latent variables in a semantic odor profile database using principal component analysis. *Chemical Senses*, 31(8):713–724.

Zhang, Y. and Sharpee, T. O. (2016). A Robust Feedforward Model of the Olfactory System. *PLoS computational biology*, 12(4):e1004850.

Zhao, S., Tian, H., Ma, L., Yuan, Y., Yu, C. R., and Ma, M. (2013). Activity-Dependent Modulation of Odorant Receptor Gene Expression in the Mouse Olfactory Epithelium. *PLoS ONE*, 8(7):e69862.

Zwicker, D., Murugan, A., and Brenner, M. P. (2016). Receptor arrays optimized for natural odor statistics. *Proceedings of the National Academy of Sciences*, 113(20):5570–5575.

A Supplementary Information

Choice of sensing matrices

We used three types of sensing matrices in this study. Two were based on experimental data, one using fly receptors (Hallem and Carlson, 2006), and one using mouse and human receptors (Saito et al., 2009); and another sensing matrix was based on randomly-generated receptor affinity profiles. These can all be either directly downloaded from our repository on GitHub, `https://github.com/ttesileanu/OlfactoryReceptorDistribution`, or generated using the code available there.

Fly sensing matrix Some of our simulations used a sensing matrix based on *Drosophila* receptor affinities, as measured by Hallem and Carlson (Hallem and Carlson, 2006). This includes the responses of 24 of the 60 receptor types in the fly against a panel of 110 odorants, measured using single-unit electrophysiology in a mutant antennal neuron. We directly used the values from Table S1 in (Hallem and Carlson, 2006), normalized to obtain the desired SNR (high for Figure 2a, low for Figure 2b, and intermediate values for Figures 2c, and 4b in the main text).

The fly data has the advantage of being more complete than the equivalent datasets in mammals, but since olfactory sensory neurons don't regenerate in the fly, it is less useful for understanding the effects of changing environments.

Mammalian sensing matrix When comparing the results from our simulation to the experimental findings from Ibarra-Soria *et al.* (Ibarra-Soria et al., 2017), we used a sensing matrix based on mouse and human receptor affinity data from (Saito et al., 2009). This was measured using heterologous expression of olfactory genes, and in total it tested 219 mouse and 245 human receptor types against 93 different odorants. However, only 52 mouse receptors and 10 human receptors exhibited detectable responses against any of the odorants, while only 63 odorants activated any receptors. From the remaining $62 \times 63 = 3906$ receptor–odorant pairs, only 335 (about 9%) showed a response, and were assayed at 11 different concentration points. In this paper, we used the values obtained for the highest concentration (3 mM).

The sparsity of the sensing matrix obtained from the Saito *et al.* (Saito et al., 2009) data makes convergence slow in our simulations. For this reason, we replaced the vanishing entries from this matrix with normally-distributed random variables, with a standard deviation of about 12% of the median value of the non-zero entries.

Random sensing matrices We generated random sensing matrices by first treating the columns of the sensing matrix (*i.e.,* the odorants) like equally-spaced points along a circle, with positions parametrized by a normalized angle $x = \theta/2\pi$. We then generated receptive fields with a Gaussian profile,

$$\phi(x) = \exp\left[-\frac{1}{2}\left(\frac{2\sin\pi(x-x_0)}{\sigma}\right)^2\right], \tag{S1}$$

where the expression in the exponent is the planar distance between a point with coordinate x and the center point of the Gaussian, with coordinate x_0. The centers x_0 for the Gaussian profiles for each of the receptors were chosen uniformly at random, and the standard deviation σ was a fixed

parameter. As a final step, we shuffled the columns of the resulting sensing matrix to remove the circular ordering of the odorants.

The parameter σ is the tuning width which appears on the x-axis in the main text in Figures 2d and 2e, where it ranges from 0.01 to 0.2. In the main text Figures 4c and 4d, the tuning parameters are 0.05 and 0.8 for top and bottom results, respectively.

Deriving the expression for the mutual information

Given that we assume a Gaussian distribution for odorant concentrations and that we approximate receptor responses as linear with additive Gaussian noise, eq. (2) in the main text, it follows that the marginal distribution of receptor responses in natural olfactory scenes is also Gaussian. Taking averages of the responses, $\langle r_a \rangle$, and of products of responses, $\langle r_a r_b \rangle$, over both the noise distribution and the odorant distribution, and using eq. (2) from the main text, we get a normal distribution of responses:

$$\mathbf{r} \sim \mathcal{N}(\mathbf{r}_0, R)\,, \tag{S2}$$

where the mean response vector $\mathbf{r}_0$ and the response covariance matrix R are given by

$$\begin{aligned} \mathbf{r}_0 &= \mathbb{K} S \mathbf{c}_0\,, \\ R &= \big[\mathbb{I} + \mathbb{K} Q\big]\,\mathbb{K}\,. \end{aligned} \tag{S3}$$

Here, as in eq. (1) in the main text, $\mathbf{c}_0$ is the mean concentration vector, Γ is the covariance matrix of concentrations, and we use the overlap matrix from eq. (5) in the main text, $Q = S\Gamma S^T$. Note that in the absence of noise, the response matrix is simply the overlap matrix Q modulated by the number of OSNs of each type, $R_{\text{noiseless}} = \mathbb{K}Q\mathbb{K}$.

The joint probability distribution over responses and concentrations, $P(\mathbf{r}, \mathbf{c})$, is itself Gaussian. To calculate the corresponding covariance matrix, we need the covariances between responses, $\langle r_a r_b \rangle - \langle r_a \rangle \langle r_b \rangle$, which are just the elements of the response matrix R from eq. (S3) above; and between concentrations, $\langle c_i c_j \rangle - \langle c_i \rangle \langle c_j \rangle$, which are the elements of the environment covariance matrix Γ, eq. (1) in the main text. In addition, we need the covariances between responses and concentrations, $\langle r_a c_i \rangle - \langle r_a \rangle \langle c_i \rangle$, which can be calculated using eq. (2) from the main text. We get:

$$(\mathbf{r}, \mathbf{c}) \sim \mathcal{N}\big((\mathbf{r}_0, \mathbf{c}_0), \Lambda\big)\,, \tag{S4}$$

with

$$\Lambda = \begin{pmatrix} R & \mathbb{K} S \Gamma \\ \Gamma S^T \mathbb{K} & \Gamma \end{pmatrix}\,. \tag{S5}$$

The mutual information between responses and odors is then given by (see the next section for a derivation):

$$I(\mathbf{r}, \mathbf{c}) = \frac{1}{2} \log \frac{\det \Gamma \det R}{\det \Lambda}\,. \tag{S6}$$

From eq. (S3) we have

$$\det R = \det(\mathbb{I} + \mathbb{K} Q) \det \mathbb{K}\,, \tag{S7}$$

and from eq. (S5),

$$\begin{aligned}\det\Lambda &= \det\begin{pmatrix} R & \mathbb{K}S\Gamma \\ \Gamma S^T\mathbb{K} & \Gamma \end{pmatrix} = \det\Gamma\cdot\det(R-\mathbb{K}S\Gamma\,\Gamma^{-1}\,\Gamma S^T\mathbb{K}) \\ &= \det\Gamma\cdot\det(\mathbb{K}+\mathbb{K}Q\mathbb{K}-\mathbb{K}S\Gamma S^T\mathbb{K}) \\ &= \det\Gamma\cdot\det\mathbb{K}\,,\end{aligned} \tag{S8}$$

where we used eq. (S3) again, and employed Schur's determinant identity (which we also derive in the next section). Thus,

$$I(\mathbf{r},\mathbf{c}) = \frac{1}{2}\log\frac{\det\Gamma\cdot\det(\mathbb{I}+\mathbb{K}Q)\cdot\det\mathbb{K}}{\det\Gamma\cdot\det\mathbb{K}} = \frac{1}{2}\log\det(\mathbb{I}+\mathbb{K}Q)\,, \tag{S9}$$

recovering the result quoted in the main text, eq. (4) in the main text.

Details regarding the derivation of the mutual information

Schur's determinant identity The identity for the determinant of a 2×2 block matrix that we used in eq. (S8) above can be derived in the following way. First, note that

$$\begin{pmatrix} A & B \\ C & D \end{pmatrix} = \begin{pmatrix} \mathbb{I} & B \\ 0 & D \end{pmatrix}\begin{pmatrix} A-BD^{-1}C & 0 \\ D^{-1}C & \mathbb{I} \end{pmatrix}. \tag{S10}$$

Now, from the definition of the determinant it can be seen that

$$\det\begin{pmatrix} A & B \\ 0 & \mathbb{I} \end{pmatrix} = \det\begin{pmatrix} A & 0 \\ C & \mathbb{I} \end{pmatrix} = \det A\,, \tag{S11}$$

since all the products involving elements from the off-diagonal blocks must necessarily also involve elements from the 0 matrix. Thus, taking the determinant of eq. (S10), we get the desired identity

$$\det\begin{pmatrix} A & B \\ C & D \end{pmatrix} = \det D\cdot\det(A-BD^{-1}C)\,. \tag{S12}$$

Mutual information for Gaussian distributions The expression from eq. (S6) for the mutual information $I(\mathbf{r},\mathbf{c})$ can be derived by starting with the fact that I is equal to the Kullback-Leibler divergence from the joint distribution $P(\mathbf{r},\mathbf{c})$ to the product distribution $P(\mathbf{r})P(\mathbf{c})$. As a first step, let us calculate the Kullback-Leibler divergence between two multivariate normals in n dimensions:

$$D = D_{\mathrm{KL}}(p\|q) = \int p(\mathbf{x})\log\frac{p(\mathbf{x})}{q(\mathbf{x})}\,d\mathbf{x}\,, \tag{S13}$$

where

$$\begin{aligned} p(\mathbf{x}) &= \frac{1}{\sqrt{(2\pi)^n\det A}}\exp\left[-\frac{1}{2}(\mathbf{x}-\mu_A)^T A^{-1}(\mathbf{x}-\mu_A)\right], \\ q(\mathbf{x}) &= \frac{1}{\sqrt{(2\pi)^n\det B}}\exp\left[-\frac{1}{2}(\mathbf{x}-\mu_B)^T B^{-1}(\mathbf{x}-\mu_B)\right]. \end{aligned} \tag{S14}$$

Plugging the distribution functions into the logarithm, we have

$$D = \frac{1}{2}\log\frac{\det B}{\det A} + \frac{1}{2}\int p(\mathbf{x})\Big[(\mathbf{x}-\mu_B)^T B^{-1}(\mathbf{x}-\mu_B) - (\mathbf{x}-\mu_A)^T A^{-1}(\mathbf{x}-\mu_A)\Big]\,d\mathbf{x}\,, \tag{S15}$$

where the normalization property of $p(\mathbf{x})$ was used. Using also the definition of the mean and of the covariance matrix, we have

$$\int p(\mathbf{x})x_i\,d\mathbf{x} = \mu_{A,i}\,, \tag{S16a}$$

$$\int p(\mathbf{x})x_i x_j\,d\mathbf{x} = A_{ij}\,, \tag{S16b}$$

which implies

$$\int p(\mathbf{x})\,(\mathbf{x}-\mu)^T C^{-1}(\mathbf{x}-\mu)\,d\mathbf{x} = \mathrm{Tr}(AC^{-1}) + (\mu_A-\mu)^T C^{-1}(\mu_A-\mu) \tag{S17}$$

for any vector μ and matrix C. Plugging this into eq. (S15), we get

$$D = \frac{1}{2}\log\frac{\det B}{\det A} + \frac{1}{2}\left[\mathrm{Tr}(AB^{-1}) - n\right] + \frac{1}{2}(\mu_A-\mu_B)^T B^{-1}(\mu_A-\mu_B)\,. \tag{S18}$$

We can now return to calculating the KL divergence from $P(\mathbf{r},\mathbf{c})$ to $P(\mathbf{r})P(\mathbf{c})$. Note that, since $P(\mathbf{r})$ and $P(\mathbf{c})$ are just the marginals of the joint distribution, the means of the variables are the same in the joint and in the product, so that the last term in the KL divergence vanishes. The covariance matrix for the product distribution is

$$\Lambda_{\mathrm{prod}} = \begin{pmatrix} R & 0 \\ 0 & \Gamma \end{pmatrix}\,, \tag{S19}$$

so the product inside the trace becomes

$$\Lambda\Lambda_{\mathrm{prod}}^{-1} = \begin{pmatrix} R & \dots \\ \dots & \Gamma \end{pmatrix}\begin{pmatrix} R^{-1} & 0 \\ 0 & \Gamma^{-1} \end{pmatrix} = \begin{pmatrix} \mathbb{I} & \dots \\ \dots & \mathbb{I} \end{pmatrix}\,, \tag{S20}$$

where the entries replaced by "…" don't need to be calculated because they drop out when the trace is taken. The sum of the dimensions of R and Γ is equal to the dimension, n, of Λ, so that the term involving the trace from eq. (S18) also drops out, leaving us with the final result:

$$I = D_{\mathrm{KL}}\left(p(\mathbf{r},\mathbf{c})\|p(\mathbf{r})p(\mathbf{c})\right) = \frac{1}{2}\log\frac{\det R\det\Gamma}{\det\Lambda}\,, \tag{S21}$$

which is the same as eq. (S6), which we used in the previous section.

Deriving the KKT conditions for the information optimum

In order to find the optimal distribution of olfactory receptors, we need to maximize the mutual information from eq. (4) in the main text, subject to constraints. Let us first calculate the gradient of the mutual information with respect to the receptor numbers:

$$\frac{\partial I}{\partial K_a} = \frac{1}{2}\frac{\partial}{\partial K_a}\log\det(\mathbb{I}+\mathbb{K}Q) = \frac{1}{2}\frac{\partial}{\partial K_a}\,\mathrm{Tr}\log(\mathbb{I}+\mathbb{K}Q)\,. \tag{S22}$$

The cyclic property of the trace allows us to use the usual rules to differentiate under the trace operator, so we get

$$\begin{aligned}\frac{\partial I}{\partial K_a} &= \frac{1}{2}\,\mathrm{Tr}\left[\frac{\partial \mathbb{K}}{\partial K_a}\left(Q^{-1}+\mathbb{K}\right)^{-1}\right] = \frac{1}{2}\sum_{b,c}\frac{\partial\left(K_b\delta_{bc}\right)}{\partial K_a}\left(Q^{-1}+\mathbb{K}\right)^{-1}_{ca} \\ &= \frac{1}{2}\left(Q^{-1}+\mathbb{K}\right)^{-1}_{aa}\,.\end{aligned} \tag{S23}$$

We now have to address the constraints. We have two kinds of constraints: an equality constraint that sets the total number of neurons, $\sum K_a = K_{\mathrm{tot}}$; and inequality constraints that ensure that all receptor abundances are non-negative, $K_a \geq 0$. This can be done using the Karush-Tucker-Kuhn (KKT) conditions, which require the introduction of Lagrange multipliers, λ for the equality constraint, and μ_a for the inequality constraints. At the optimum, we must have:

$$\begin{aligned}\frac{\partial I}{\partial K_a} &= \frac{1}{2}\lambda\frac{\partial}{\partial K_a}\left(\sum_b K_b - K_{\mathrm{tot}}\right) - \sum_b \mu_b \frac{\partial}{\partial K_a}K_b \\ &= \lambda - \mu_a\,,\end{aligned} \tag{S24}$$

where the Lagrange multipliers for the inequality constraints, μ_a, must be non-negative, and must vanish unless the inequality is saturated:

$$\begin{aligned}\mu_a &\geq 0\,, \\ \mu_a K_a &= 0\,.\end{aligned} \tag{S25}$$

Put differently, if $K_a > 0$, then $\mu_a = 0$ and $\partial I/\partial K_a = \lambda/2$; while if $K_a = 0$, then $\partial I/\partial K_a = \lambda/2 - \mu_a \leq \lambda/2$. Combined with eq. (S23), this yields

$$\begin{cases}(Q^{-1}+\mathbb{K})^{-1}_{aa} = \lambda\,, & \text{if } K_a > 0, \text{ or} \\ (Q^{-1}+\mathbb{K})^{-1}_{aa} < \lambda\,, & \text{if } K_a = 0.\end{cases} \tag{S26}$$

The magnitude of λ is set by imposing the normalization condition $\sum K_a = K_{\mathrm{tot}}$.

Deriving the high total neuron number approximation

Suppose we are in the regime in which the total number of neurons is large, and in particular, each of the abundances K_a is large. Then we can perform an expansion of the expression appearing in the KKT equations from eq. (S26):

$$(A+\mathbb{K})^{-1} = \mathbb{K}^{-1}(\mathbb{I}+A\mathbb{K}^{-1})^{-1} \approx \mathbb{K}^{-1}(\mathbb{I}-A\mathbb{K}^{-1})\,, \tag{S27}$$

where we used the notation $A = Q^{-1}$. This implies

$$\lambda \approx \frac{1}{K_a} - \frac{A_{aa}}{K_a^2}\,. \tag{S28}$$

This quadratic equation has only one large solution, and it is given approximately by

$$K_a \approx \frac{1}{\lambda} - A_{aa}\,. \tag{S29}$$

Combined with the normalization constraint, $\sum_a K_a = K_{\text{tot}}$, this recovers eq. (7) from the main text.

In the main text we also showed that eq. (7) can give a useful approximation of receptor abundances even for intermediate SNR regimes. In that case, some of the right-hand-sides in eq. (S29) might become negative. We can improve the approximation by clipping all values at 0,

$$K_a \approx \max\Big(0, \frac{1}{\lambda} - A_{aa}\Big) . \tag{S30}$$

The value for the Lagrange multiplier λ might then need to be adjusted to keep the total number of neurons $\sum_a K_a$ fixed at K_{tot}.

First receptor type to be activated

When there is only one active receptor, $K_x = K_{\text{tot}}$, $K_{a\neq x} = 0$, the KKT conditions from eq. (S26) are automatically satisfied. The receptor that is activated first can be found in this case by calculating the information $I(\mathbf{r}, \mathbf{c})$ using eq. (4) from the main text while assuming an arbitrary index x for the active receptor, and then finding $x = x^*$ that yields the maximum value. Without loss of generality, we can permute the receptor indices such that $x = 1$. We have, when $K_1 = K_{\text{tot}}$,

$$\begin{aligned} I_1(\mathbf{r}, \mathbf{c}) &= \frac{1}{2} \operatorname{Tr} \log(\mathbb{I} + \mathbb{K}Q) = \frac{1}{2} \log\det(\mathbb{I} + \mathbb{K}Q) \\ &= \frac{1}{2} \log \begin{vmatrix} 1 + K_{\text{tot}}Q_{11} & K_{\text{tot}}Q_{12} & \cdots & K_{\text{tot}}Q_{1M} \\ 0 & 1 & & 0 \\ \vdots & & \ddots & \\ 0 & 0 & \cdots & 1 \end{vmatrix} \\ &= \frac{1}{2} \log\big(1 + K_{\text{tot}}Q_{11}\big) . \end{aligned} \tag{S31}$$

Thus, in general, the information when only receptor type x is activated is given by

$$I_x(\mathbf{r}, \mathbf{c}) = \frac{1}{2} \log\big(1 + K_{\text{tot}}Q_{xx}\big) , \tag{S32}$$

which implies that information is maximized when x matches the receptor corresponding to the highest diagonal value of the overlap matrix Q,

$$x^* = \arg\max Q_{xx} . \tag{S33}$$

Another way to think of this result is by employing the usual expression for the capacity of a single Gaussian channel, and then finding the channel that maximizes this capacity.

Random environment matrices

Generating plausible olfactory environments is difficult because so little is known about natural odor scenes. However, it is reasonable to expect that there will be some strong correlations. This could, for instance, be due to the fact that an animal's odor is composed of several different odorants in fixed proportions, and thus concentrations of these odorants will be correlated.

To generate covariance matrices that have a non-trivial correlation structure, we used a modified form of an algorithm based on partial correlations (Lewandowski et al., 2009). The basic idea is that there is a recurrence relation that allows one to eliminate the conditioning variables one by one, so that a set of unconditioned correlations can be obtained by recursively processing the partial correlations.

The distributions from which the partial correlations are drawn in (Lewandowski et al., 2009) are beta distributions with parameters that depend on the order of the correlations. These are chosen such that the resulting matrices provide a uniform sampling in the space of correlation matrices. However, this leads to samples that are close to diagonal and thus not particularly suitable for modeling olfactory environments. By simply keeping the beta distribution parameters equal to a given fixed value, $\alpha = \beta = \text{const}$, instead of changing depending on the order of the partial correlations, we can instead obtain matrices with a tunable amount of correlation. More specifically, large values of β lead to almost uncorrelated environments, while small values lead to environments with strong correlations between odorant concentrations. We found this modified algorithm in an entry on the question-and-answer website `Stack Exchange`, at `https://stats.stackexchange.com/q/125020`. This method generates a correlation matrix, in which all the variances are equal to 1. Random variances are then drawn from a lognormal distribution and the rows and columns are multiplied by their square roots, generating a final covariance matrix. The detailed code is available on GitHub, at `https://github.com/ttesileanu/OlfactoryReceptorDistribution`.

When comparing the qualitative results from our model against experiments in which the odor environment changes (Ibarra-Soria et al., 2017), we used small perturbations of the initial and final environments to estimate error bars on receptor abundances. To generate a perturbed covariance matrix, $\tilde{\Gamma}$, from a starting matrix Γ, we first took the matrix square root: a symmetric matrix M, which obeys

$$\Gamma = MM^T \equiv M^2 \,. \tag{S34}$$

We then perturbed M by adding normally-distributed *i.i.d.* values to its elements,

$$\tilde{M}_{ij} = M_{ij} + \sigma\eta_{ij} \,, \tag{S35}$$

and recreated a covariance matrix by multiplying the perturbed square root with its transpose,

$$\tilde{\Gamma} = \tilde{M}\tilde{M}^T \,. \tag{S36}$$

This approach ensures that the perturbed matrix $\tilde{\Gamma}$ remains a valid covariance matrix—symmetric and positive-definite—which wouldn't be guaranteed if the random perturbation was added directly to Γ. We chose the magnitude σ of the perturbation so that the error bars in our simulations are of comparable magnitude to those in the experiments.

Deriving the dynamical model

To turn the maximization requirement into a dynamical model, we turn to a gradient ascent argument. Given the current abundances K_a, we demand that they change in proportion to the corresponding components of the information gradient, plus a Lagrange multiplier to impose the constraint on the total number of neurons:

$$\dot{K}_a = 2\alpha\left(\frac{\partial I}{\partial K_a} - \lambda\right) = \alpha\big[\big(Q^{-1} + \mathbb{K}\big)^{-1}_{aa} - \lambda\big] \,. \tag{S37}$$

The brain does not have direct access to the overlap matrix Q, but it could measure the response covariance matrix R from eq. (S3). Thus, we can write the dynamics as

$$\begin{aligned}\dot{K}_a &= \alpha\Big\{\big[Q(\mathbb{I}+\mathbb{K}Q)^{-1}\big]_{aa} - \lambda\Big\} \\ &= \alpha\Big\{\big[\mathbb{K}^{-1}(R\mathbb{K}^{-1}-\mathbb{I})\mathbb{K}R^{-1}\big]_{aa} - \lambda\Big\} \\ &= \alpha\Big\{K_a^{-1} - \lambda - R_{aa}^{-1}\Big\}\,.\end{aligned} \tag{S38}$$

These equations do not yet obey the non-negativity constraint on the receptor abundances. The divergence in the K_a^{-1} term would superficially appear to ensure that positive abundances stay positive, but there is a hidden quadratic divergence in the response covariance term, R_{aa}^{-1}; see eq. (S3). To ensure that all constraints are satisfied while avoiding divergences, we multiply the right-hand-side of eq. (S38) by K_a^2, yielding

$$\dot{K}_a = \alpha\big[K_a - K_a^2\big(\lambda + R_{aa}^{-1}\big)\big]\,, \tag{S39}$$

which is the same as eq. (8) from the main text.

If we keep the Lagrange multiplier λ constant, the asymptotic value for the total number of neurons K_{tot} will depend on the statistical structure of olfactory scenes. If instead we want to enforce the constraint $\sum K_a = K_{\text{tot}}$ for a predetermined K_{tot}, we can promote λ itself to a dynamical variable,

$$\frac{d\lambda}{dt} = \beta\left[\sum_a K_a - K_{\text{tot}}\right], \tag{S40}$$

where β is another learning rate. Provided that the dynamics of λ is sufficiently slow compared to that of the neuronal populations K_a, this will tune the experience-independent component of the neuronal death rate until the total population stabilizes at K_{tot}.

Multiple glomeruli with the same affinity profile

In mammals, the axons from neurons expressing a given receptor type can project to anywhere from 2 to 16 different glomeruli. Here we show that in our setup, information transfer only depends on the total number of neurons of a given type, and not on the number of glomeruli to which they project.

The key observation is that mutual information, eq. (3) in the main text, is unchanged when the responses and/or concentrations are modified by monotonic transformations. In particular, linear transformations of the responses do not affect the information values. Suppose that we have a case in which two receptors p and q have identical affinities, so that $S_{pi} = S_{qi}$ for all odorants i. We can then form linear combinations of the corresponding glomerular responses,

$$\begin{aligned} r_+ &= r_p + r_q = (K_p + K_q)\sum_i S_{pi}c_i + \eta_p\sqrt{K}_p + \eta_q\sqrt{K}_q\,, \\ r_- &= K_q r_p - K_p r_q = \eta_p K_q\sqrt{K}_p - \eta_q K_p\sqrt{K}_q\,, \end{aligned} \tag{S41}$$

and consider a transformation that replaces (r_p, r_q) with (r_+, r_-). Since r_- is pure noise, *i.e.,* it does not depend on the concentration vector $\mathbf{c}$ in any way, it has no effect on the mutual information.

We have thus shown that the amount of information that M receptor types contain about the environment when two of the receptors have identical affinity profiles is the same as if there were only $M-1$ receptor types. The two redundant receptors can be replaced by a single one with an abundance equal to the sum of the abundances of the two original receptors. (Remember that in eq. (2) in the main text we had assumed that the responses are normalized such that the variance of η is unity. This is automatically satisfied for the r_+ response from eq. (S41) because the sum of two Gaussian variables with the same mean is Gaussian itself and has a variance equal to the sum of the variances of the two variables. This means that the noise term in eq. (S41) is equivalent to $\eta_+\sqrt{K_p+K_q}$, with $\eta_+ \sim \mathcal{N}(0,1)$.)

Interpretation of diagonal elements of inverse overlap matrix

In the main text we saw that the diagonal elements of the inverse overlap matrix Q^{-1}_{aa} were well-correlated with the abundances of OSNs K_a. Recall that the overlap matrix was defined as $Q = S\Gamma S^T$, where S is the sensing matrix, and Γ is the environment covariance matrix (see eq. (1) and eq. (2) in the main text). In the main text, we suggested that a possible explanation for this correlation is based on the relation between inverse covariance matrices (also called precision matrices) and partial correlations.

More specifically, as noted around eq. (S3) above, the overlap matrix Q and the response covariance matrix are related: in particular, Q is equal to R when there is a single receptor of each type ($K_a = 1$) and there is no noise ($\eta = 0$ in eq. (2) in the main text). Thus, the inverse overlap matrix $A = Q^{-1}$ is effectively a precision matrix. Diagonal elements of a precision matrix are inversely related to the corresponding diagonal elements of the corresponding covariance matrix, but they are also monotonically-related to goodness-of-fit parameters that show how well each variable can be linearly predicted from all the others. Since receptor responses that either do not fluctuate much or whose values can be guessed based on the responses from other receptors are not very informative, we would expect that abundances K_a are low when the corresponding diagonal elements of the inverse overlap matrix A_{aa} are high, which is what we see. In the following we give a short derivation of the connection between the diagonal elements of precision matrices and goodness-of-fit parameters.

Let us thus work in the particular case in which there is one copy of each receptor and there is no noise, so that $Q = R$, *i.e.*, $Q_{ij} = \langle r_i r_j\rangle - \langle r_i\rangle\langle r_j\rangle$. Without loss of generality, we focus on calculating the first diagonal element of the inverse overlap matrix, A_{11}, where $A = Q^{-1}$. For notational convenience, we will also denote the mean-centered first response variable by $y \equiv r_1 - \langle r_1\rangle$, and the subsequent ones by $x_a \equiv r_{a+1} - \langle r_{a+1}\rangle$. Then the covariance matrix Q can be written in block form

$$Q = \begin{pmatrix} \langle y^2\rangle & \langle y\mathbf{x}^T\rangle \\ \langle y\mathbf{x}\rangle & M \end{pmatrix}, \tag{S42}$$

where M is

$$M = \langle \mathbf{x}\mathbf{x}^T\rangle\,. \tag{S43}$$

Using the definition of the inverse together with Laplace's formula for determinants, we get

$$A_{11} = \frac{\det M}{\det Q}\,. \tag{S44}$$

Using the Schur determinant identity (derived above) on the block form (eq. (S42)) of the matrix Q,

$$\begin{aligned} A_{11} &= \frac{\det M}{\det M \cdot \det\left[\langle y^2\rangle - \langle y\mathbf{x}^T\rangle M^{-1}\langle y\mathbf{x}\rangle\right]} \\ &= \frac{1}{\langle y^2\rangle - \langle y\mathbf{x}^T\rangle M^{-1}\langle y\mathbf{x}\rangle}\,, \end{aligned} \tag{S45}$$

where we used the fact that the argument of the second determinant is a scalar.

Now, consider approximating the first response variable y by a linear function of all the others:

$$y = \mathbf{a}^T\mathbf{x} + q\,, \tag{S46}$$

where q is the residual. Note that we do not need an intercept term because we mean-centered our variables, $\langle y\rangle = \langle x\rangle = 0$. Finding the coefficients $\mathbf{a}$ that lead to a best fit (in the least-squares sense) requires minimizing the variance of the residual, and a short calculation yields

$$\mathbf{a}^* = \arg\min_{\mathbf{a}} \langle q\rangle^2 = \arg\min_{\mathbf{a}} (y - \mathbf{a}^T\mathbf{x})^2 = M^{-1}\langle y\mathbf{x}\rangle\,, \tag{S47}$$

where M is the same as the matrix defined in eq. (S43).

The coefficient of determination ρ^2 is defined as the ratio of explained variance to total variance of the variable y,

$$\begin{aligned} \rho^2 &= \frac{\langle(\mathbf{a}^{*T}\mathbf{x})^2\rangle}{\langle y^2\rangle} = \frac{\mathbf{a}^{*T}\langle\mathbf{x}\mathbf{x}^T\rangle\mathbf{a}^*}{\langle y^2\rangle} = \frac{\langle y\mathbf{x}^T\rangle M^{-1}MM^{-1}\langle y\mathbf{x}\rangle}{\langle y^2\rangle} \\ &= \frac{\langle y\mathbf{x}^T\rangle M^{-1}\langle y\mathbf{x}\rangle}{\langle y^2\rangle}\,. \end{aligned} \tag{S48}$$

Comparing this to eq. (S45), we see that

$$A_{11} = \frac{1}{\langle y^2\rangle}\frac{1}{1-\rho^2}\,, \tag{S49}$$

showing that indeed the diagonal elements of the precision matrix are monotonically-related to the goodness-of-fit parameter ρ^2 that indicates how well the corresponding variable can be linearly predicted by all the other variables. In addition, the inverse dependence on the variance of the response $\langle y\rangle^2$ shows that variables that do not fluctuate much (low $\langle y\rangle^2$ and thus high A_{11}) tend to have low abundances.